Cellular Physiology and Biochemistry

Cell Physiol Biochem 2026;60:503-517
DOI: 10.33594/000000885
Published online: 1 September 2026
Accepted: 16 August 2026

Original Paper

Tumor Destructive Mechanical Impulse (TMI) Treatment of Solid Tumors. Part IV: Palliative Management of Painful Bone Metastases, Pain Relief – and Beyond

Axel Erich Theuera Stella Exner[b] Ioannis Thomas[c] Florian Lang[d] John Warlick[e] John David Mullins[f] Thomas K. Eigentler[a] Gerhard Franz Walter[g]

[a]Department of Dermatology, Venerology and Allergology, Charité University Hospital, Berlin, Germany, [b]Pediatrician's Office, Marktoberdorf, Germany, [c]EDOEAP (Unified Journalistic Organization of Supplementary Insurance and Health), Athens, Greece, [d]Institute of Immunology, University of Duisburg-Essen, Essen, Germany, [e]Immunosonics, Talking Rock, GA, USA, [f]Shepherd Center Wound Clinic, Piedmont Atlanta Hospital, Atlanta, GA, USA, [g]International Neuroscience Institute, Hannover, Germany

Key Words
Bone metastases • Palliative pain management • Tumor-destructive mechanical impulses • Simulation-guided therapy • Focused shock waves • Immunological abscopal effect

Abstract
Background/Aims: Bone metastases are a frequent and highly debilitating complication of advanced malignancies and are associated with severe pain, structural instability and loss of functional capacity. Radiotherapy, systemic antineoplastic therapy, bone-targeted agents and interventional techniques remain the clinical standard, yet a relevant proportion of patients experience only incomplete or transient pain relief. Non-invasive focal approaches are therefore being explored. Tumor-destructive mechanical impulses (TMI) – an umbrella term for shock-type, high-strain acoustic pulses generated by electrohydraulic, electromagnetic or piezoelectric systems – have a long safety record in musculoskeletal medicine and are increasingly investigated in oncology. We report the palliative use of TMI in patients with painful bone metastases. ***Methods:*** Patient-specific DICOM data were segmented using Simpleware ScanIP® and imported into ANSYS SpaceClaim for geometry preparation, enabling coupled device-tissue simulations under clinical pressure wave forms; the resulting anatomical models were simulated in ANSYS Explicit Dynamics. In parallel, DICOM data were processed using MATLAB®/TABLIN and converted into OnScale® for high-frequency pressure wave propagation analysis, predicting pressure fields, focal volumes and attenuation through bone. The outputs of the numerical solution of the finite element (FEM) propagation models comprise total energy, energy flux density, pulse count and frequency, and the

Prof. Dr.-Ing. habil. A. Erich Theuer
Department of Dermatology, Venerology and Allergology, Charité University Hospital, Berlin, Germany.
Tel. +49-162-3884554, E-Mail: prof.theuer@gmail.com

optimal placement of the TMI applicator. TMI was applied within individual healing attempts in patients in whom conventional therapy had failed. ***Results:*** In two patients with metastatic prostate carcinoma described in detail, and in thirteen further patients with bone metastases, TMI applied to metastatic bone lesions was followed by relief of periosteal pain. In both index patients, follow-up Ga-68-PSMA PET-CT showed marked regression of the osseous lesions. Treatments were tolerated without device-related complications; in one patient the piezoelectric technique was not tolerated and was replaced by the electrohydraulic technique. ***Conclusion:*** TMI treatment combines direct mechanotransduction with controlled cavitation, potentially disrupting tumor cells and microvasculature and inducing features of immunogenic cell death. In the patients reported here, palliative TMI treatment was associated with pain relief and radiographic tumor regression, including observations compatible with a possible immunological abscopal response. These observations derive from uncontrolled individual healing attempts under concomitant systemic therapy and require prospective confirmation.

Introduction

We have recently proposed the treatment of malignant solid tumors by tumor-destructive mechanical impulses (TMI) as a novel physical approach to cancer therapy [1-3]. In patients with advanced painful bone metastases, TMI can additionally be used in a purely palliative setting for pain relief. The present paper is confined to this palliative indication.

Bone metastases occur frequently in advanced breast, prostate and lung cancer and are major drivers of morbidity through almost intractable pain, pathological fractures and reduced mobility. Current guidelines for the interventional management of cancer-associated pain comprise neurolysis by injection, neuromodulation including targeted drug delivery and spinal cord stimulation, vertebral tumor ablation and augmentation, palliative radiotherapy and surgical techniques [4]. Opioids remain the pharmacological mainstay for moderate-to-severe pain associated with bone metastasis [5]. Despite these established approaches, 30-40% of patients experience incomplete or only transient pain relief [5-7].

Here we report the results of palliative TMI treatment addressing almost intractable pain and functional impairment caused by bone metastases. TMI is an umbrella term for shock-type, high-strain acoustic pulses generated by electrohydraulic, electromagnetic or piezoelectric systems, with a long safety record in musculoskeletal medicine. Originally developed for lithotripsy, subsequently established for tendinopathies and bone healing, and historically termed extracorporeal shock wave therapy [8], TMI translates these tissue-regenerative and analgesic effects [9-14] to oncology, in the present context to the palliative treatment of painful bone metastases.

Materials and Methods

TMI generator technologies

TMI refers to the therapeutic delivery of short, high-amplitude acoustic pulses to tissue. TMI generators include electrohydraulic, electromagnetic and piezoelectric systems; all deliver steep pressure fronts with a tensile tail that can induce intracellular cavitation within tumor cells (Fig. 1). The generator and applicator technologies have been described in detail by our group in a previous publication [2]. Technical improvements of TMI for application in patients suffering from malignant tumors have been designed and patented by the first author [15].

Biophysical considerations and targeting

Bone metastases are usually located at the bone marrow border, a region near the interface of the trabecular spongiosa and the cortical compacta. The biophysical properties of the tissue layers to be traversed by TMI have been described by our group in a previous publication [3]. The TMI target volume contains metastatic cells, osteoclasts and stromal cells and responds to mechanical stimuli, which makes it accessible to mechanotransduction (Fig. 2).

Energy losses at impedance mismatches and wavefront scattering necessitate careful trajectory selection and soft-focus strategies covering the lesion with adequate safety margins (Fig. 3).

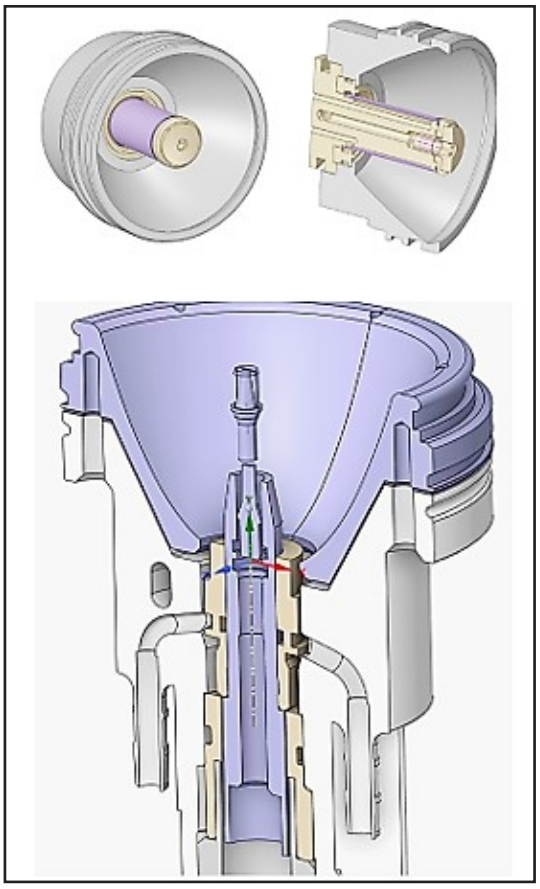

Fig. 1. Above: Geometric configuration of the electromagnetic shock wave applicator; a Lorentz-force membrane- or coil-driven acoustic pulse is launched into a reflector; cavitation can be controlled via energy and pulse profiling. Below: Sectional view of the electrohydraulic shock wave applicator with focusing geometry; spark-gap discharge in water creates a plasma bubble and a shock wave, focused by an ellipsoidal reflector with a broad focal zone and a strong cavitation propensity.

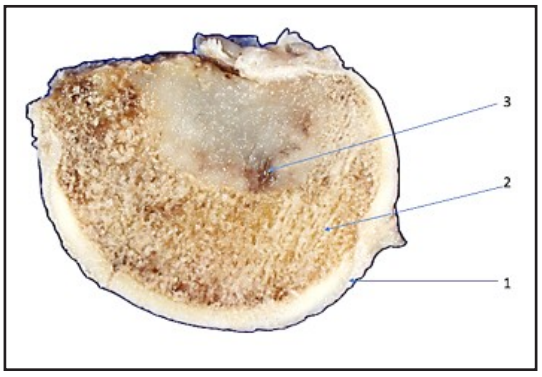

Fig. 2. Bone disc for experimental evaluation of treatment parameters. 1 – zona compacta; 2 – zona spongiosa; 3 – bone metastasis in the complex microenvironment between trabeculae and bone marrow.

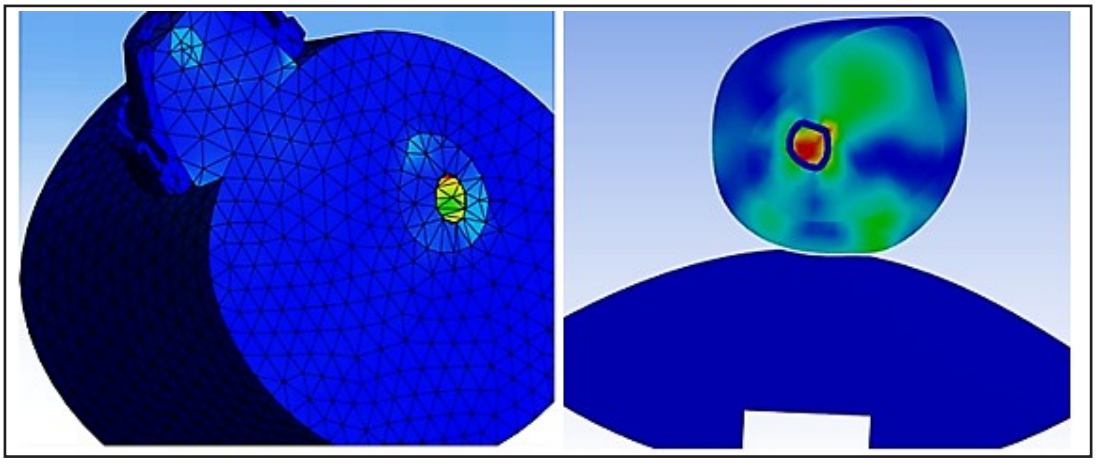

Fig. 3. Left: Computational simulation for the determination of optimal treatment parameters targeting the bone metastasis in question. Right: Simulation of acoustic pressure distribution in bone; the red zone indicates focal stress at the metastasis.

Patient-specific planning workflow

To ensure patient safety and reproducibility, patient-specific DICOM (Digital Imaging and Communications in Medicine) data were segmented using Simpleware ScanIP® (Synopsys Inc.) and subsequently imported into ANSYS SpaceClaim (ANSYS® SpaceClaim, version 2024.R2, ANSYS Inc.) for geometry preparation, enabling coupled device-tissue simulations under clinical pressure wave forms. The resulting anatomical models (Fig. 4) were then simulated in ANSYS Explicit Dynamics (ANSYS® Mechanical, version 2024.R2, ANSYS Inc.).

In parallel, DICOM data were processed using MATLAB®/TABLIN and converted into OnScale® (formerly PZFlex, OnScale Inc.), an explicit time-domain solver designed for high-frequency pressure wave propagation analysis in complex biological media, suitable for predicting pressure fields, focal volumes and attenuation through bone. The outputs of the numerical solution of the finite element (FEM) propagation models comprise total energy, energy flux density, pulse count and frequency, and the optimal placement of the TMI applicator (Figures 5 and 6).

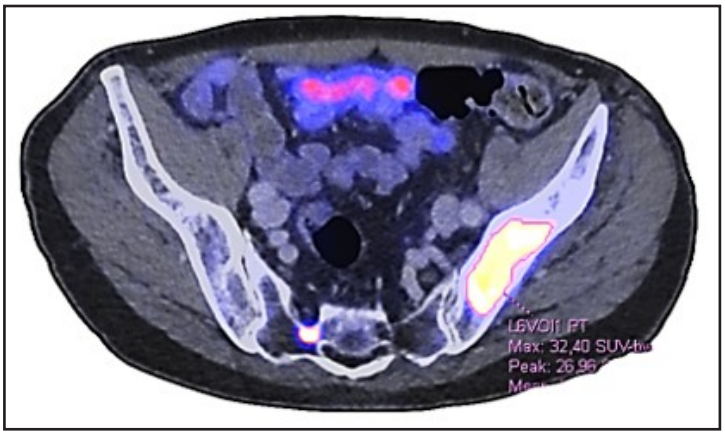

Fig. 4. Geometry representation of DICOM data of a patient with prostate carcinoma suffering from multiple painful bone metastases (white) in the iliac and sacral bones.

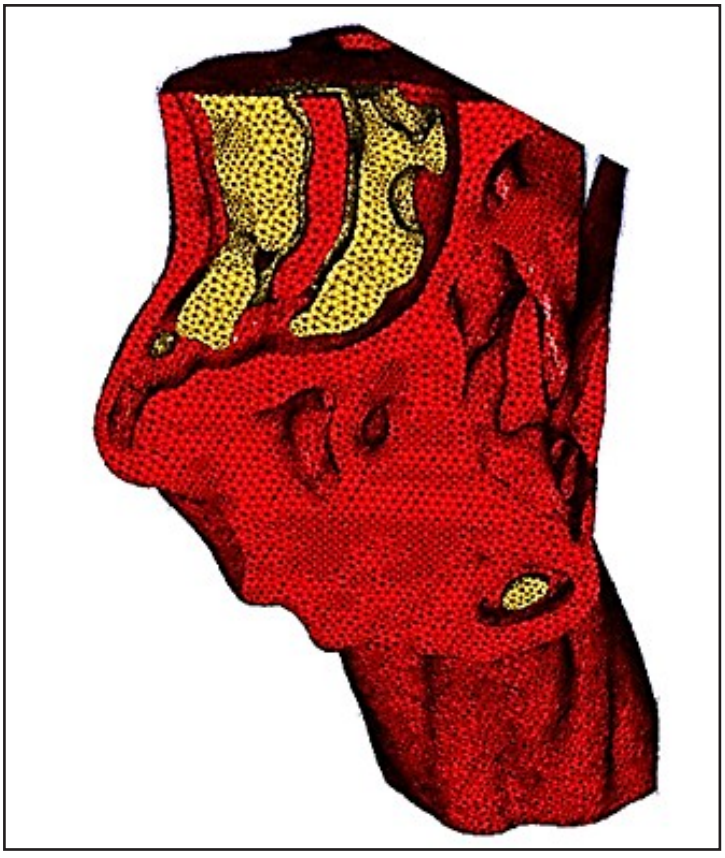

Fig. 5. Finite element (FEM) mesh of a femur with tumor infiltration (yellow).

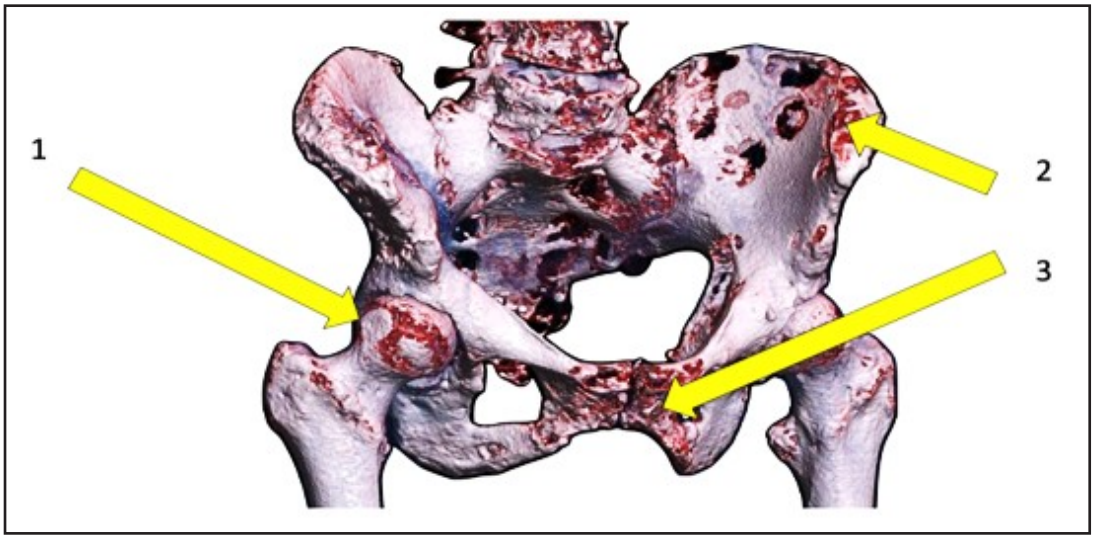

Fig. 6. Individual 3D MRI/CT DICOM determination of positioning options for the electrohydraulic TMI applicator, targeting metastases (brown) of 1 – caput femoris, 2 – os ilium, 3 – os pubis (arrows).

Treatment delivery

The technical options for TMI generator technologies (electrohydraulic, EH; electromagnetic, EM; piezoelectric, PZ) have been described by our group in a previous publication [3]. In patients, each treatment session comprised focused EH, EM or PZ pulses at a frequency of 2-4 Hz and an energy flux density in the range of 0.17-0.27 mJ/mm^2 using the electrohydraulic OrthoGold100® device (OrthoGold100®, MTS Medical UG) [16] and the piezoelectric PiezoWave2 device, and up to 1.24 mJ/mm^2 using the PiezoLith 3000Plus device (Richard Wolf GmbH) [17], titrated to tolerance. Standard contraindications (air-filled lung fields, major neurovascular bundles, growth plates) were respected. Analgesia was administered as needed; no incisions or implants were required.

Applicator positioning

Individual 3D MRI/CT DICOM data determined the positioning options for the TMI applicator in each patient (Fig. 6).

Setting and patient selection

TMI was not applied within a clinical trial. All treatments reported here were performed as individual healing attempts in patients with advanced metastatic disease in whom established therapeutic options had been exhausted or were not tolerated. Because of the unfavorable prognosis, the option of palliative TMI treatment was discussed with each patient in detail, including its investigational character, the absence of controlled efficacy data and the alternatives available. All patients provided written informed consent to the individual healing attempt and to the use of their de-identified clinical data for publication. In all patients, individual DICOM/FEM data were acquired to define patient-specific treatment parameters, and easily accessible osseous metastases were selected as targets. No prospective protocol, no predefined endpoints and no systematic instrument-based pain or quality-of-life assessment were applied; the observations reported below are therefore descriptive.

Results

Two patients are presented in detail, followed by a summary of thirteen further patients.

Patient A

A 58-year-old patient suffered from prostate carcinoma with osseous metastases causing periosteal pain. Biopsy revealed an acinar adenocarcinoma with extensive neuroendocrine differentiation; Gleason score primary pattern 4 + secondary pattern 5 = 9. Multiple sclerosis had been present for eight years and increasingly impaired the patient through gait instability and balance disturbance.

Androgen deprivation therapy with bicalutamide and a GnRH analogue was initiated. Concurrently, palliative radiotherapy was administered to the thoracic vertebrae T8 and T12, which were heavily affected by metastases. The anti-hormonal regimen was subsequently changed to apalutamide and triptorelin. In addition, denosumab was administered, a RANK ligand (receptor activator of nuclear factor kappa-B ligand, RANKL) inhibitor that prevents the formation and function of osteoclasts by blocking the RANKL/RANK interaction.

Over a two-year period of pharmacological treatment, the PSA level fell from an initial 120 µg/L to 1.47 µg/L. Following palliative radiotherapy to the prostate, the PSA level fell to 1,02 µg/L. A Ga-68-PSMA PET-CT scan showed that the extent of osseous involvement throughout the axial skeleton – specifically the thoracic vertebrae, the right ilium and the right femur – was unchanged compared with previous radiological findings.

In addition, infiltration of the sigmoid colon by the primary tumor was suspected, a process that had shown a progressive trend over the preceding two years. Retroperitoneal and iliac lymph node involvement showed a slightly regressive trend, and the onset of mesenteric involvement was radiologically suspected. As the patient was considered unsuitable for docetaxel chemotherapy because of the concomitant multiple sclerosis, the feasibility and indication for radioligand LuPSMA therapy were discussed. At this stage of the disease, in addition to continued anti-hormonal therapy, palliative TMI treatment was administered to the skeleton. The PSA level before TMI treatment was 0.86 µg/L.

The primary targets were the right ilium and the 8th thoracic vertebra, treated concomitantly; the sites were selected on basis of the previously acquired PET-CT images. Because of the patient's neurological condition, it became apparent immediately at the start of treatment that the piezoelectric technique was poorly tolerated; consequently, the entire series of treatment sessions was conducted using the electrohydraulic OrthoGold100® device with the focused OE50 applicator. Over a period of 18 weeks, 22 TMI sessions were administered at regular intervals. Given the patient's reduced tolerance, each session comprised 800 pulses to the thoracic spine region (T8) and 1, 000 pulses to the region of the right pelvic bone, at a frequency of 2 Hz and an energy flux density typically set at 0.19 mJ/mm^2, on isolated occasions increased to 0.25 mJ/mm^2.

Six months after the start of TMI treatment, a follow-up Ga-68-PSMA PET-CT revealed marked regression of all metastatic osseous lesions and moderate regression of the retroperitoneal and iliac lymph nodes, whereas the primary tumor site and its extensions remained unchanged. In view of the regression and the now low level of PSMA expression, which did not exceed hepatic uptake, the findings no longer met the methodological criteria for radioligand therapy (Fig. 7).

Following a two-month interval, TMI treatment was administered at intervals of 3 to 4 weeks. Concomitant with the regression of bone metastases, the patient became free of periosteal pain. After TMI treatment, the PSA level had declined to 0.38 µg/L.

The multidisciplinary uro-oncology Tumor Board Prostata of the Comprehensive Cancer Center at the University of Ulm summarized the findings as follows: Lymph nodes typical of metastases in the retroperitoneal, iliac and inferior mesenteric artery distribution, some previously enlarged, now showed reduced and only moderate PSMA expression. Osseous lesions typical of metastases showed marked regression and only low PSMA expression,

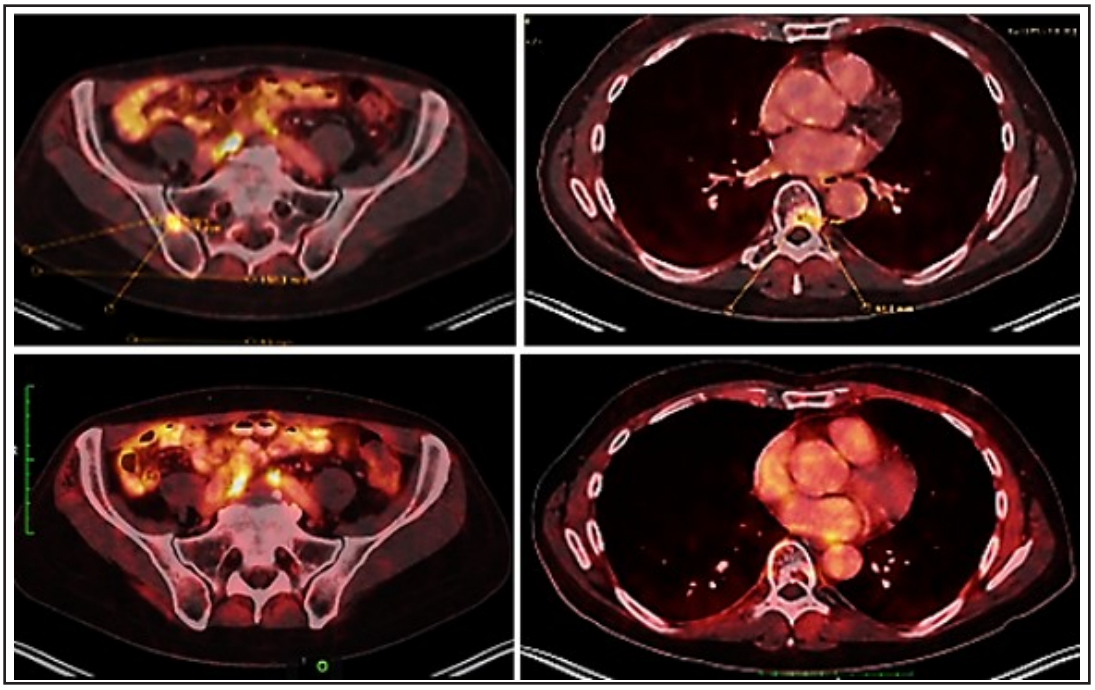

Fig. 7. PSMA PET-CT showing osseous metastases in the ilium and the 8th thoracic vertebra before TMI treatment (above) and regression of the osseous metastases six months after the start of TMI treatment (below).

predominantly sclerotic and unchanged, with some lytic components, for example in the T8 vertebra near the posterior margin. The collapse of the L4 vertebral body affecting the superior and inferior endplates and the depression of the T12 superior endplate were unchanged, without posterior margin displacement, and no clearly stability-compromising osseous lesion was evident. Unchanged sclerotic, disseminated, non-PSMA-expressing osseous lesions throughout the axial skeleton and the proximal extremities were interpreted as low-activity osteoblastic lesions. There was no evidence of parenchymal or pulmonary organ metastases. The board determined this to indicate a good therapeutic response, particularly with respect to the osseous lesions and the lymph node metastases. The immune status assessment performed eight months after the start of therapy showed evidence of biologically active, systemic immunomodulation. The slight reduction in the $CD4^+$ T-cell count was not interpreted as clinically relevant immunosuppression but rather as redistribution and functional demand associated with an activated immune response. The thymic reserve was within the age-appropriate reference range, indicating preserved capacity for T-cell generation. Immune activation was documented by an increased proportion of pre-activated $CD25^+$ T cells, a pattern suggesting antigen-specific stimulation such as would be expected following TMI-induced tumor-antigen release. TMI also triggers danger-associated molecular patterns (DAMPs), which can initiate dendritic cell activation and T-cell priming. Analysis of $CD8^+$ T-cell subpopulations revealed a shift towards terminally differentiated effector T cells alongside low-normal proportions of naive and effector memory cells and reduced central memory cells, a profile characteristic of sustained or repeated antigen exposure and indicative of an active cytotoxic response against tumor antigens. The predominance of terminal effector cells correlates with the capacity for direct tumor cell lysis and with the potential for systemic abscopal effects. The proportion of regulatory T cells ($CD4^+/CD25^{++}$/CD127low) was normal, indicating that neither compensatory nor therapy-induced immune tolerance had developed; the low absolute Treg count is explained by the overall reduction in $CD4^+$ cell numbers and does not constitute an independent pathological finding. This is of clinical relevance, since expansion of regulatory T cells is among the most common causes

of failure of immunomodulatory therapies. Overall, the immune profile showed no signs of exhaustion but rather functional activation of the cellular immune system, with particular emphasis on the $CD8^+$ effector axis. As these findings derive from a single patient under concomitant systemic therapy, they are hypothesis-generating and cannot establish causality.

Patient B

A 64-year-old patient suffered from prostate carcinoma with osseous metastases causing periosteal pain. No surgical intervention had been performed and the patient declined chemotherapy, but androgen deprivation therapy was administered. At this stage of the disease, in addition to continued anti-hormonal therapy, palliative TMI treatment directed at the bone metastases was initiated. Within nine months the patient received four treatment cycles comprising 23 TMI sessions in total.

During the first cycle the patient received eight sessions within four weeks using the PiezoWave2 device. Different gel pads (GP 40, GP 50, GP 60) were used to determine the penetration depth. Adapted to the patient's pain sensitivity, sessions comprised 1,000 to 2,000 pulses to the sacral metastases at a frequency of 3 to 4 Hz and an energy flux density between 0.17 and 0.27 mJ/mm^2. The treatments were well tolerated.

After an interval of two months, the second cycle comprised five sessions within five days using the OrthoGold100® device with the highly focused applicator. In addition, an anti-hormonal regimen with the GnRH antagonist degarelix was initiated. Adapted to his pain sensitivity, the treatment sessions involved delivering an increased number of pulses from 500 to 2,000 to the sacral metastases. These were applied at a frequency of 2 Hz, with an energy flux density that typically increased slowly up to 0.27 mJ/mm^2.

A follow-up Ga-68-PSMA PET-CT revealed marked regression of all metastatic osseous lesions in the sacral region (Fig. 8).

The third cycle comprised five sessions within five days using the OrthoGold100® device. Sessions comprised 800 pulses, increased to 2, 000 pulses, to the sacral metastases at a frequency of 2 Hz and an energy flux density slowly increased up to 0.27 mJ/mm^2. During one session the energy flux density was increased to 0.478, then 0.578 and eventually 0.678 mJ/mm^2. The treatments were well tolerated.

After a further interval of two months, the fourth cycle again comprised five sessions within five days, using a combined application of the PiezoWave2 device (GP 40 and GP 50) and the OrthoGold100® device with the highly focused applicator. Sessions comprised 1,000 pulses to the sacral metastases at a frequency of 2 Hz and an energy flux density slowly increased up to 0.27 mJ/mm^2. For the final session, a combined application of the PiezoWave2 device and the OrthoGold100® device with a less focused applicator was used; the therapeutic focal field was correspondingly larger and deeper, with a penetration depth of up to 120 mm and a width of up to 25 mm; for the final session with the less focused applicator, the energy flux density was up to 0.18 mJ/mm^2.

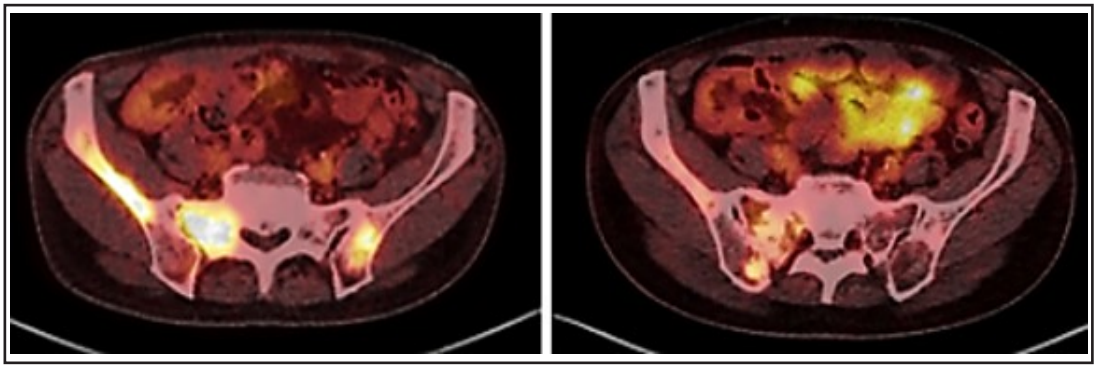

Fig. 8. PSMA PET-CT of osseous metastases (white) before TMI treatment (left) and regression of the osseous metastases five months after the start of TMI treatment (right).

The PSA level fell from an initial 2.3 µg/L to 0.21 µg/L. Concomitant with the regression of the bone metastases, the patient became free of periosteal pain.

Further patients

Thirteen further patients with bone metastases reported relief of pain within weeks after TMI treatment. Ten of these patients suffered from prostate carcinoma as the primary tumor, two from malignant melanoma and one from renal cell carcinoma. Technical TMI treatment parameters are summarized (Table 1). Three patients were treated with the PiezoLith 3000Plus device [17] which allows for an enhanced energy flux density of up to 1.24 mJ/mm^2.

Follow-up in this group is heterogeneous and was not conducted according to a predefined schedule. Five patients were observed for five years or more after the last TMI treatment. One patient died of an influenza infection, so that the further course under TMI treatment cannot be assessed in this case. Clinical information regarding magnitude and duration of pain relief, analgesic requirements, mobility, or functional improvement was not collected systematically, so that the subjective feeling indicated by the respective patient is stated for pain relief (Table 2).

The patients who received treatment for severe pain with opioids (e.g. tramadol, fentanyl) or strong prescription painkillers (e.g. novaminsulfon) before TMI treatment, did not need any longer strong medication after TMI treatment.

In none of the cases reported, device-related complications occurred.

Table 1. Treatment parameters of thirteen patients with bone metastases reporting pain relief after palliative TMI treatment. F – frequency, EFD – energy flux density, PL3000+ – PiezoLith 3000Plus device, OG100 – OrthoGold100® device, PW2 – PiezoWave2 device

No.	Age (yrs)	Sex	Primary tumor	TMI sessions (n)	F	EFD (mJ/mm^2)	Pulses (n)	Device
1	72	m	Prostate carcinoma	4	2	1.24	4000	PL3000+
2	68	m	Prostate carcinoma	4	2	1.24	4000	PL3000+
3	65	m	Prostate carcinoma	6	2	0.3–0.7	4000/4000	OG100/PW2
4	65	m	Prostate carcinoma	6	2	0.3–0.7	4000/4000	OG100/PW2
5	70	m	Prostate carcinoma	7	2	0.3–0.7	4000/4000	OG100/PW2
6	77	m	Prostate carcinoma	8	2	0.3–0.7	4000/4000	OG100/PW2
7	66	m	Prostate carcinoma	8	2	0.3–0.7	4000/4000	OG100/PW2
8	71	m	Prostate carcinoma	12	2	0.3	6000	OG100
9	69	m	Prostate carcinoma	12	2	0.3–0.7	4000/4000	OG100/PW2
10	83	m	Prostate carcinoma	14	2	0.3–0.7	4000/4000	OG100/PW2
11	70	f	Malignant melanoma	8	2	0.3–0.7	4000/4000	OG100/PW2
12	69	m	Malignant melanoma	18	2	0.3–0.7	4000/4000	OG100/PW2
13	64	f	Renal cell carcinoma	4	2	1.24	4000	PL3000+

Table 2. Summarized clinical results of palliative TMI treatment for pain relief

No.	Age (yrs)	Sex	Primary tumor	Duration until pain relief after TMI treatment	Lomg term pain relief after TMI treatment
1	72	m	Prostate carcinoma	3 days	Permanently pain-free
2	68	m	Prostate carcinoma	3 days	Permanently pain-free
3	65	m	Prostate carcinoma	7 days	Improved, remaining moderate pain
4	65	m	Prostate carcinoma	3 days	Improved, remaining distinct pain
5	70	m	Prostate carcinoma	7 days	Improved, remaining moderate pain
6	77	m	Prostate carcinoma	7 days	Improved, remaining moderate pain
7	66	m	Prostate carcinoma	3 days	Improved, remaining moderate pain
8	71	m	Prostate carcinoma	2 days	Improved, remaining moderate pain
9	69	m	Prostate carcinoma	14 days	Improved, remaining moderate pain
10	83	m	Prostate carcinoma	3 days	Permanently pain-free
11	70	f	Malignant melanoma	3 days	Permanently pain-free
12	69	m	Malignant melanoma	14 days	Improved, remaining moderate pain
13	64	f	Renal cell carcinoma	3 days	Permanently pain-free

Discussion

Palliative approach to pain relief

Particular caution is required for the interpretation of the imaging findings because all patients received concomitant systemic therapy, and previous radiotherapy was also relevant in one index patient. Androgen deprivation therapy, apalutamide, denosumab, degarelix, and prior radiotherapy can independently affect PSA levels, PSMA expression, sclerosis of osseous lesions, and pain. Accordingly, radiological regression should not be attributed to TMI alone.

TMI treatment is increasingly explored as a non-invasive method for pain relief in cancer patients [18] and for direct antitumor effects [19-21], although the mechanisms of the direct effects are still not completely understood by the therapists [21]. In the patients reported here, relief of periosteal pain and improvement of mobility were observed without escalation of opioid therapy.

Pathophysiological considerations and mechanisms inferred from the broader focused shock-wave literature suggest the assumption that TMI may in the same way as reported achieve analgesic effects through stimulation and modulation of nociceptive mediators, namely activation of descending pain inhibitory pathways, alteration of sensory nerve activity and upregulation of anti-inflammatory mediators such as nitric oxide and endorphins [22]. In the treated metastasis and in the surrounding tissue, angiogenesis and tissue regeneration are induced via upregulation of vascular endothelial growth factor (VEGF), endothelial nitric oxide synthase (eNOS) and bone morphogenetic proteins (BMPs), promoting neovascularization and osteogenesis. Osteogenesis through stimulation of osteoblast proliferation and differentiation supports stabilization of the bone microarchitecture while simultaneously suppressing osteoclastogenesis, thus shifting bone remodeling towards

osteoblast activity [23, 24]. At osteolytic sites, regenerative signaling may promote sclerosis and microarchitectural stabilization. These effects appear most pronounced near the marrow border, where cellular density and vascularization are high.

And beyond: immunological abscopal effect of TMI treatment

The hypothesis of direct antitumor activity, immunogenic cell death, systemic immune activation, and of an abscopal effect is supported by the previously presented animal experiment, in which TMI treatment alone also produced these effects, and by the distinct abscopal effect in TMI treated patients suffering from metastatic malignant melanoma [1].

Beyond histotripsy (high-intensity focused ultrasound, HIFU) tumor ablation, the ability of low-intensity TMI treatment to induce 'soft parameter' mechanical stress, with or without cavitation bubble formation, offers a hitherto unexploited opportunity to disrupt tumor architecture and stimulate anti-tumor immunity, although the specific mechanisms of this enhancement remain to be established [25] (Fig. 9).

Low-intensity TMI treatment induces overstretching of tumor cell membranes, leading to disruptive impairment of tumor cells and thereby unmasking previously disguised tumor antigens, so that tumor cells become identifiable to the adaptive immune system. Unmasked tumor antigens are taken up by immature dendritic cells, which mature and present the antigens to naive T cells in the lymph nodes. The resulting effector T cells are distributed via blood vessels, including tumor vessels. Once the CD8 receptor recognizes a tumor cell, cytotoxic $CD8^+$ T cells are activated and selectively destroy tumor cells of the primary tumor and of metastases [26]. Second and subsequent TMI treatments, delivered before complete re-stretching of the cell structures, cause additional disruptive stretching without necessarily causing immediate cell destruction. Repetitive TMI treatments thus evoke repeated and extended unmasking of antigens of still viable tumor cells, activating the adaptive immune system and potentially inducing an abscopal effect [27].

The dual action of TMI treatment – mechanotransductive regeneration and analgesia on the one hand, cavitation-mediated tumor disruption on the other – may alleviate pain, stabilize bone and initiate systemic anti-tumor immunity. TMI treatment combined with tumor-binding cavitation agents may transform the tumor into an immunogenic focus, acting not only through immediate immunological effects but potentially also as an in-situ vaccine that recruits and activates the adaptive immune system for durable anti-tumor responses.

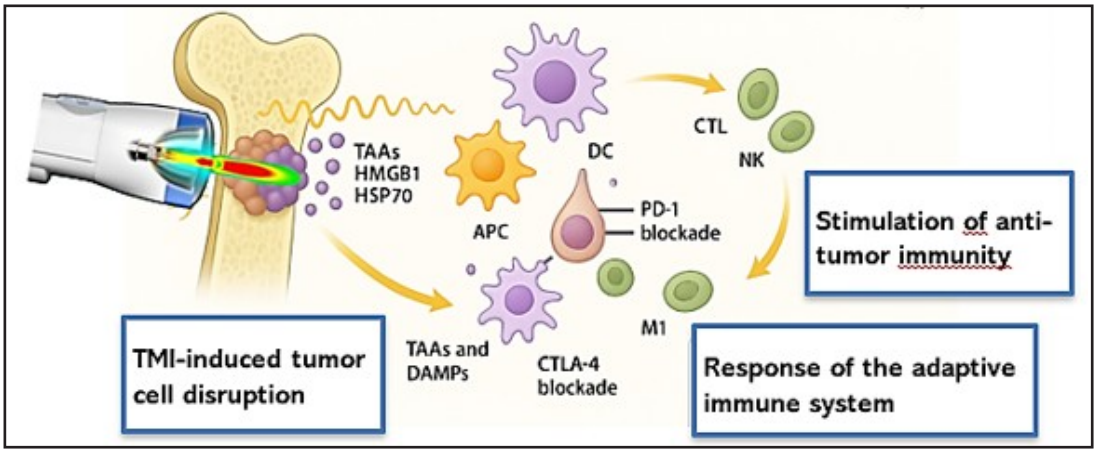

Fig. 9. Localized immune activation in bone marrow following focused TMI therapy. TAA – tumor-associated antigen; HMGB1 – high mobility group box 1 protein; HSP70 – heat shock protein 70; DAMPs – danger-associated molecular patterns; APC – antigen-presenting cell; DC – dendritic cell; CTL – cytotoxic T lymphocyte; NK – natural killer cell; M1 – activated macrophage; PD1 – programmed cell death protein 1; CTLA-4 – cytotoxic T lymphocyte-associated antigen-4.

Our observations are compatible with the hypothesis that repeated TMI treatments induce a systemic immune response without significant immune dysregulation or tolerance, a pattern consistent with the clinical observation of disease stabilization in these patients.

Limitations

The interpretation of the imaging findings requires special caution because all patients received concomitant systemic therapy, and previous radiotherapy was also relevant in Patient A. Androgen deprivation therapy, apalutamide, denosumab, degarelix, and prior radiotherapy can independently affect PSA levels, PSMA expression, sclerosis of osseous lesions, and pain. Accordingly, radiological regression cannot be attributed to TMI treatment alone.

The observations reported here derive from uncontrolled individual healing attempts in a small, heterogeneous group of patients. There was no control group, no randomization and no blinding. Pain relief and quality of life were not assessed with validated instruments such as the visual analogue scale, the numerical rating scale or established quality-of-life questionnaires, and opioid consumption was not quantified; the statements on pain relief therefore rest on clinical documentation rather than on standardized measurement. In Patient A the primary TMI target T8 had previously been irradiated.

Adverse events were not recorded systematically, so the absence of reported complications does not constitute a formal safety assessment; the observation that the piezoelectric technique was not tolerated by Patient A indicates that tolerability differs between generator technologies. However, no device-related complications were documented in this series. Finally, follow-up intervals differ between patients and were not defined in advance.

Perspectives

Translational TMI studies should prospectively measure immune responses (for example $CD8^+$ infiltration and DAMP kinetics) and evaluate dendritic cell priming, and should integrate TMI with immunotherapy where appropriate. Prospective controlled clinical trials are required to define dose-response relationships (energy flux density, pulse number, focal strategy), the number and spacing of sessions, validated pain and quality-of-life endpoints, and safety in irradiated or structurally compromised bone.

Conclusion

TMI treatment is a non-invasive and, in the patients reported here, well-tolerated palliative option for the management of pain caused by bone metastases. With careful consideration of the limitations discussed, the following mechanisms are proposed:

1. *Analgesic effects via hyperstimulation and modulation of nociceptive mediators:* Activation of descending pain inhibitory pathways, alteration of sensory nerve activity, and upregulation of anti-inflammatory mediators such as nitric oxide and endorphins.
2. *Angiogenesis and tissue regeneration via upregulation of VEGF, eNOS and BMPs:* Increased expression of vascular endothelial growth factor and bone morphogenetic proteins, and promotion of neovascularization.
3. *Osteogenesis via stimulation of osteoblast proliferation and differentiation:* Potential stabilization of the bone microarchitecture with simultaneous suppression of osteoclastogenesis, shifting bone remodeling towards osteoblast activity. At osteolytic sites, regenerative signaling may promote sclerosis and microarchitectural stabilization. These effects appear most pronounced near the marrow border, where cellular density and vascularization are high.
4. *Immunomodulation via features of immunogenic cell death with DAMP release and dendritic cell priming:* TMI treatment can disrupt fragile tumor microvasculature, reduce perfusion and mechanically injure tumor cells via cavitation microjets. Specific

tumor antigens are unmasked by microtrauma and cavitation-related strain on tumor cells, and apoptotic and immune signaling in tumor-associated stromal cells is stimulated by mechanotransduction. We suggest the interpretation that modulation of the tumor microenvironment by TMI treatment may induce an abscopal effect.

These mechanisms are inferred from the established biology of focused shock waves and from the observations reported here; they require confirmation in prospective controlled trials before palliative TMI treatment can be recommended for routine clinical use.

Acknowledgements

We thank F. Zengerling, Department of Urology/Comprehensive Cancer Center, University of Ulm, Germany, S. Rausch, Department of Urology, University of Tübingen, Germany, and T. Todenhöfer, Studienpraxis für klinische Phase I-IV-Studien urologischer Erkrankungen, Nürtingen, Germany, for their valuable clinical advice and support.

Ethics statement

The experimental TMI treatment of patients was not performed within a clinical trial and has been approved by the Ethics Committee at the Medical Faculty of the Eberhard Karls University of Tübingen (PNR150/2019BO2). All patients were adults and were TMI-treated after established therapeutic options had been exhausted or were not tolerated. All patients were informed of the purpose of the treatment, of its investigational character, of the available alternatives and of the risks and potential benefits, and all provided written informed consent to the individual healing attempt and to the use of their de-identified clinical data for publication. The retrospective evaluation and publication of the clinical data were performed in accordance with the Declaration of Helsinki and with the rules of the responsible ethics committees.

Author contributions

A.E. Theuer and G.F. Walter, with the scientific support of F. Lang, established the biological feasibility of TMI treatment of cancer. I. Thomas evaluated tumor cell reactions to shock wave treatment and provided clinical background for the design of the application devices. S. Exner, T.K. Eigentler, J. Warlick and J.D. Mullins helped to transform the concept into clinical practice. G.F. Walter wrote the manuscript. All authors approved of the manuscript.

Data availability

The de-identified clinical data supporting the findings of this report are available from the corresponding author upon reasonable request.

Disclosure Statement

A.E. Theuer was supported by Zentrales Innivationsprogramm Mittelstand (grant number ZF4803001BA9). A.E. Theuer is co-inventor and holder of U.S. Patent No. 11, 752, 365 B2 covering a device for the treatment of malignant disease by tumor-destructive mechanical impulses [15]. J. Warlick is affiliated with Immunosonics, Talking Rock, GA, USA. The remaining authors declare that they have no competing interests.

References

1 Theuer AE, Thomas I, Lang F, Borkmann M, Mullins JD, Eigentler TK, Walter GF: Tumor destructive mechanical impulse (TMI) treatment of solid tumors. Part I: Animal experiments, clinical application and immunological abscopal effect. Cell Physiol Biochem 2025;59:800-810.

2 Theuer AE, Schierbaum N, Niessner H, Sinnberg TW, Schäffer TE, Lang F, Mullins JD, Eigentler TK, Walter GF: Tumor destructive mechanical impulse (TMI) treatment of solid tumors. Part II: Biomechanics, computational simulation, technical generator and applicator design, and physiological effect. Cell Physiol Biochem 2026;60:30-43.
3 Theuer AE, Exner S, Thomas I, Lang F, Mullins JD, Warlick J, Strassmann G, Eigentler TK, Walter GF: Tumor destructive mechanical impulse (TMI) treatment of solid tumors. Part III: Transcranial application, immune profile, blood-brain barrier, neuroprotection, neuromodulation and neurostimulation. Cell Physiol Biochem 2026;60:175-188.
4 Aman MM, Mahmoud A, Deer T, Sayed D, Hagedorn JM, Brogan SE, Singh V, Gulati A, Strand N, Weisbein J, Goree JH, Xing F, Valimahomed A, Pak DJ, El Helou A, Ghosh P, Shah K, Patel V, Escobar A, Schmidt K, Shah J, Varshney V, Rosenberg W, Narang S: The American Society of Pain and Neuroscience (ASPN) best practices and guidelines for the interventional management of cancer-associated pain. J Pain Res 2021;14:2139-2164.
5 Zhang H, Paice J, Portenoy R, Bruera E, Reid MC, Bao Y: Prescription opioids dispensed to patients with cancer with bone metastasis: 2011-2017. Oncologist 2021;26:e1890-e1892.
6 Behroozian T, Navarro I, Hoskin P, Johnstone C, Recht A, Menten J, Oldenburger E, van der Linden Y, van der Velden JM, Nguyen QN, Simone CB 2nd, Johnstone P, Lutz S, Milton L, Andratschke N, Willmann J, Kazmierska J, Spałek M, Chow E, Raman S: Update on the systematic review/meta-analysis of uncomplicated bone metastases treated with external beam radiation. Radiother Oncol 2022;174:109-110.
7 Hofbauer LC, Bozec A, Rauner M, Jakob F, Perner S, Pantel K: Novel approaches to target the microenvironment of bone metastasis. Nat Rev Clin Oncol 2021;18:488-505.
8 D'Agostino MC, Frairia R, Romeo P, Amelio E, Berta L, Bosco V, Gigliotti S, Guerra C, Messina S, Messuri L, Moretti B, Notarnicola A, Maccagnano G, Russo S, Saggini R, Vulpiani MC, Buselli P: Extracorporeal shockwaves as regenerative therapy in orthopedic traumatology: a narrative review from basic research to clinical practice. J Biol Regul Homeost Agents 2016;30:323-332.
9 Zelle BA, Gollwitzer H, Zlowodzki M, Bühren V: Extracorporeal shock wave therapy: current evidence. J Orthop Trauma 2010;24(Suppl 1):S66-S70.
10 De la Corte-Rodríguez H, Román-Belmonte JM, Rodríguez-Damiani BA, Vázquez-Sasot A, Rodríguez-Merchán EC: Extracorporeal shock wave therapy for the treatment of musculoskeletal pain: a narrative review. Healthcare (Basel) 2023;11:2830.
11 Zdravkovic A, Mickel M, Crevenna R: Successful application of focused extracorporeal shockwave therapy for plantar fasciitis in patients suffering from metastatic breast cancer. Support Care Cancer 2021;29:4187-4190.
12 Wang CJ, Huang HY, Pai CH: Shock wave-enhanced neovascularization at the tendon-bone junction: an experiment in dogs. J Foot Ankle Surg 2002;41:16-22.
13 Wang Z, Wang Z, Wu F: Application of extracorporeal shockwave to regulate subchondral bone homeostasis through tumor necrosis factor-α/hypoxia-inducible factor-1α/vascular endothelial growth factor signaling pathway in treatment of talus bone marrow edema. Medicine (Baltimore) 2024;103:e40228.
14 Ren P, Wang Z, Liang Z, Xia S, Yuan X, Zhou F, Liu X: Radial extracorporeal shock wave therapy for pain and function in adults with knee osteoarthritis: protocol for a placebo-controlled, randomized clinical trial. Trials 2025;26:139.
15 Theuer AE, Theuer I: Device for treating malignant diseases with the help of tumor-destructive mechanical pulses (TMI). U.S. Patent No. 11, 752, 365 B2, 2023.
16 MTS Medical UG. OrthoGold100®, https://www.mts-medical.com/de/orthopaedics (accessed July 21, 2026).
17 Richard Wolf GmbH. https://www.richard-wolf.com/de/disziplinen/stosswellen/ (accessed July 21, 2026).
18 Crevenna R, Mickel M, Keilani M: Extracorporeal shock wave therapy in the supportive care and rehabilitation of cancer patients. Support Care Cancer 2019;27:4039-4041.
19 Grushina TI, Orlov II: Udarno-volnovaya terapiya v onkologii: *in vitro*, *in vivo*, reabilitatsiya [Shock wave therapy in oncology: *in vitro*, *in vivo*, rehabilitation]. Vopr Kurortol Fizioter Lech Fiz Kult 2022;99:58-65.
20 Hosano N, Moosavi-Nejad Z, Hide T, Hosano H: Focused shock waves and inertial cavitation release tumor-associated antigens from renal cell carcinoma. Ultrason Sonochem 2024;111:107078.
21 Zhang X, Ran C, Song Q, Lv G: Extracorporeal shock waves effectively suppress colorectal cancer proliferation and growth. Sci Rep 2025;15:9769.

22 Mariotto S, Cavalieri E, Amelio E, Ciampa AR, de Prati AC, Marlinghaus E, Russo S, Suzuki H: Extracorporeal shock waves: from lithotripsy to anti-inflammatory action by NO production. Nitric Oxide 2005;12:89-96.
23 Wang CJ, Wang FS, Yang KD, Weng LH, Hsu CC, Huang CS, Yang LC: Shock wave therapy induces neovascularization at the tendon-bone junction. A study in rabbits. J Orthop Res 2003;21:984-989.
24 Zhang Z, Ma Y, Guo S, He Y, Bai G, Zhang W: Low-intensity pulsed ultrasound stimulation facilitates *in vitro* osteogenic differentiation of human adipose-derived stem cells via up-regulation of heat shock protein (HSP)70, HSP90, and bone morphogenetic protein (BMP) signaling pathway. Biosci Rep 2018;38:BSR20180087.
25 Bulner S, Prodeus A, Gariepy J, Hynynen K, Goertz DE: Enhancing checkpoint inhibitor therapy with ultrasound stimulated microbubbles. Ultrasound Med Biol 2019;45:500-512.
26 Raskov H, Orhan A, Christensen JP, Gögenur I: Cytotoxic CD8+ T cells in cancer and cancer immunotherapy. Br J Cancer 2021;124:359-367.
27 Nabrinsky E, Macklis J, Bitran J: A review of the abscopal effect in the era of immunotherapy. Cureus 2022;14:e29620.